

Understanding Ligand Distributions in Modified Particle and Particlelike Systems

Ilhem F. Hakem,[†] Anna M. Leech,[‡] Jermaine D. Johnson,[‡] Scott J. Donahue,[‡] Jeremy P. Walker,[‡] and Michael R. Bockstaller^{*†}

Department of Materials Science and Engineering, Carnegie Mellon University, 5000 Forbes Avenue, Pittsburgh, Pennsylvania 15213, United States, and ICx Technologies, 2240 William Pitt Way, Pittsburgh, Pennsylvania 15238, United States

Received August 9, 2010; E-mail: bockstaller@cmu.edu

Abstract: Chemical modification of nanoparticles or particlelike systems is ubiquitously being used to facilitate specific pharmaceutical functionalities or physicochemical attributes of nanocrystals, proteins, enzymes, or other particlelike systems. Often the modification process is incomplete and the functional activity of the product depends upon the distribution of functional ligands among the different particles in the system. Here, the distribution function describing the spread of ligands in particlelike systems undergoing partial modification reactions is derived and validated against a conjugated enzyme model system by use of matrix-assisted laser desorption ionization time-of-flight mass spectrometry (MALDI-TOF). The distribution function is shown to be applicable to describe the distribution of ligands in a wide range of particlelike systems (such as enzymes, dendrimers, or inorganic nanocrystals) and is used to establish guidelines for the synthesis of uniformly modified particle systems even at low reaction efficiencies.

Introduction

Much of the promise of emerging technologies involving nanoparticlelike systems is related to the ability to modify the surface of a particle entity in order to facilitate a specific functionality such as site-selective binding, biocompatibility, or other desired physico- and biochemical properties.^{1–3} In general, the required functionality is not readily available after preparation of the primary particle species but has to be introduced by means of subsequent chemical modification. For example, the preparation of inorganic and organic nanoparticles for therapeutic and diagnostic purposes typically involves the coupling of site-specific docking groups such as monoclonal antibodies or biocompatible polymer chains onto the particle surface.^{4–7}

Similarly, the conjugation of polymers such as poly(ethylene glycol) (PEG) to “biological nanoparticles” such as proteins, enzymes, or viruses is widely being used to improve the pharmacokinetics and stability of novel therapeutic agents.⁸ Often the chemical reaction that is fundamental to the coupling process is incomplete and results in only partial functionalization of the available sites.^{9–11} Under these circumstances, knowledge of the distribution of reacted sites among the various particles is highly desirable, since a particle system in which the number of functional ligands is narrowly distributed about the average value can differ dramatically in its activity from a corresponding system with a broader diversity of functionalized particles.^{12,13} Understanding of the statistical characteristics of site distributions in chemical modification processes involving particlelike species is thus a critical prerequisite for the realization of tailored particle-based technologies. However, although the relevance of site distributions in determining particle functionality has been widely recognized (in particular in the biomedical domain), to date only qualitative understanding about the nature of distributions associated with incomplete coupling reactions has been achieved.^{14,15} This can be attributed both to the experimental

[†] Carnegie Mellon University.

[‡] ICx Technologies.

- (1) Di Marco, M.; Shamsuddin, S.; Razak, K. A.; Aziz, A. A.; Devaux, C.; Borghi, E.; Levy, L.; Sadun, C. *Int. J. Nanomed.* **2010**, *5*, 37–49.
- (2) Peer, D.; Karp, J. M.; Hong, S.; FaroKhazad, O. C.; Margalit, R.; Langer, R. *Nat. Nanotechnol.* **2007**, *2*, 751–760.
- (3) (a) Bartneck, M.; Keul, H.; Singh, S.; Czaja, K.; Bornemann, J.; Bockstaller, M.; Moeller, M.; Zwadlo-Klarwasser, G.; Groll, J. *ACS Nano* **2010**, *4*, 3073–3086. (b) Boisselier, E.; Diallo, A. K.; Salmon, L.; Ornelas, C.; Ruiz, J.; Astruc, D. *J. Am. Chem. Soc.* **2010**, *132*, 2729–2742. (c) Ojha, S.; Beppler, B.; Dong, H.; Matyjaszewski, K.; Garoff, S.; Bockstaller, M. R. *Langmuir* **2010**, *26*, 13210–13215.
- (4) Wu, W.; Hsiao, S. C.; Carrico, Z. M.; Francis, M. B. *Angew. Chem., Int. Ed.* **2009**, *48*, 9493–9497.
- (5) Medintz, I. L.; Uyeda, H. T.; Goldman, E. R.; Mattoussi, H. *Nat. Mater.* **2005**, *4*, 435–446.
- (6) Heath, J. R.; Davis, M. E. *Annu. Rev. Med.* **2008**, *59*, 251–265.
- (7) (a) Zickich, D.; Borovok, N.; Kotlyar, A. *Bioconjugate Chem.* **2010**, *21*, 544–547. (b) Heegaard, P. M. H.; Boas, U.; Sorensen, N. S. *Bioconjugate Chem.* **2010**, *21*, 405–418. (c) Astruc, D.; Boisselier, E.; Ornelas, C. *Chem. Rev.* **2010**, *110*, 1857–1959. (d) Boas, U.; Heegaard, P. M. H. *Chem. Soc. Rev.* **2004**, *33*, 43–63. (e) Krupkova, A.; Cermak, J.; Walterova, Z.; Horsky, J. *Macromolecules* **2010**, *43*, 4511–4519.

(8) Joralemon, M. J.; McRae, S.; Emrick, T. *Chem. Commun.* **2010**, *46*, 1377–1393.

(9) Veronese, F. M. *Biomaterials* **2001**, *22*, 405–417.

(10) Roberts, M. J.; Bentley, M. D.; Harris, J. M. *Adv. Drug Delivery Rev.* **2002**, *54*, 459–476.

(11) Casanova, D.; Giaume, D.; Moreau, M.; Martin, J.-L.; Gacoin, T.; Boilot, J.-P.; Alexandrou, A. *J. Am. Chem. Soc.* **2007**, *129*, 12592–12593.

(12) Jevsevar, S.; Kunstelj, M.; Poreka, V. G. *Biotechnol. J.* **2010**, *5*, 113–128.

(13) Gao, W.; Liu, W.; Mackay, J. A.; Zalutsky, M. R.; Toone, E. J.; Chilkoti, A. *Proc. Natl. Acad. Sci. U.S.A.* **2009**, *106*, 15231–15236.

(14) Mullen, D. G.; Fang, M.; Desai, A.; Baker, J. R., Jr.; Orr, B. G.; Banaszak Holl, M. M. *ACS Nano* **2010**, *4*, 657–670.

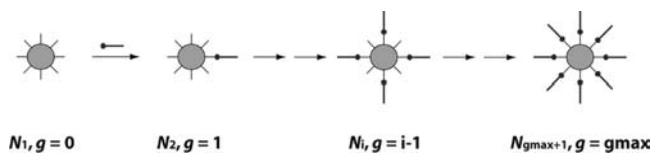


Figure 1. Illustration of the generic reaction process for the modification of particlelike systems. The total number of reactive sites per particle is g_{\max} . The coupling of functional ligands is assumed to proceed by a sequence of irreversible coupling reactions with equal and constant rate, that is, interactions between surface-bound ligands are neglected (see text for details).

challenge of differentiating particle species with minor differences in the number of reacted sites in a mixed particle system and to the lack of mechanism-based statistical models to predict and evaluate site distributions. In this paper we derive an analytical expression that captures the site distribution associated with incomplete modification reactions of particle systems using a kinetic analysis of the generic reaction process. The distribution is shown to exhibit excellent agreement with experimental data on conjugated enzyme model systems (as well as literature data on various other particlelike systems) and to provide guidelines for the synthesis of uniformly modified particle systems even at low reaction efficiencies.

Results and Discussion

Theoretical Description of Ligand Distributions. In the following discussion the term “particle” will be used to represent a generic particlelike entity such as an inorganic nanocrystal, dendrimer, protein, enzyme, or virus with a given number of reactive sites g_{\max} exposed at the “particle surface”. These particles are assumed to undergo a chemical modification process during which “functional ligands” are being bound to the particle surface (in reality these functional ligands could correspond to, for example, biocompatible polymer chains or residues for site-specific binding). The number of ligands bound to the particle surface at any given instant is denoted g . Particle and modification process are assumed to fulfill the following conditions: (1) the total number of reactive sites capable of binding a functional ligand per particle surface (g_{\max}) remains constant during the course of the reaction. (2) The modification occurs by a sequence of kinetically identical coupling reactions.¹⁶ (3) Each coupling step is considered irreversible. (4) The ligand species is present in excess quantity such that its concentration can be considered constant. Figure 1 illustrates the modification process that will be analyzed in the following section.

In the trivial case of highly efficient modification reactions, each step of the reaction sequence can be considered complete, thus resulting in a fully functionalized particle product. However, in the (more typical) case of incomplete reactions, a distribution of the number of functional ligands among the various particles in the system is expected. In the latter case the total efficiency ε of the modification process may be defined as $\varepsilon = \langle g \rangle / g_{\max}$.

where $\langle g \rangle$ denotes the average number of functional ligands per particle after completion of the modification process ($\varepsilon \ll 1$ for incomplete modification processes). The distribution of functional ligands among the various particles in the system may be derived from an analysis of the reaction sequence illustrated in Figure 1. Let N_1, N_2, N_3 , etc., denote the number of particle species that possess zero, one, two, etc., functional ligands coupled to the particle surface. By use of this notation, the rate of consumption of (pristine) particle species N_1 from the reaction system can be written as

$$\frac{dN_1}{dt} = -k_{g_{\max}} N_1 \quad (1)$$

The rate is proportional to g_{\max} , the number of available reactive sites before modification as well as the kinetic constant k that will depend on the conditions of the reaction (such as temperature or solvent). The solution to the problem of ligand distributions is independent of the detailed nature of k , provided that k is identical for each step of the reaction sequence. According to assumption 2, the rate describing the formation of (monofunctionalized) particle species N_2 is then given as

$$\frac{dN_2}{dt} = k_{g_{\max}} N_1 - k(g_{\max} - 1) N_2 \quad (2)$$

where the first term describes the rate of formation of N_2 from N_1 and the second term describes the rate of consumption of species N_2 in the process of formation of N_3 . Note that the rate of consumption of a particle species is proportional to the respective number of available reactive sites and decreases with each functional ligand that is being coupled to the particle surface. In general, the rate of formation of a particle with g functional ligands will thus be given as

$$\frac{dN_{g+1}}{dt} = k\{[g_{\max} - (g - 1)]N_g - (g_{\max} - g)N_{g+1}\} \quad (3)$$

From the reaction sequence shown in Figure 1 (in conjunction with assumption 1 above), it follows that the total rate of disappearance of reactive sites is given by $-(ds/dt) = k \sum_g [(g_{\max} - g)N_{g+1}] = kn_p(g_{\max} - \langle g \rangle) \cong kn_p g_{\max}$, where s denotes the number of reactive sites at any given time, n_p is the total number of particles in the system, and the last relation requires that the modification is inefficient as described above (the latter restriction is not severe, as the result will be shown to be appropriate for efficiencies in excess of 40%). Defining the ratio of reacted sites at time t to the total initial number of sites as $\nu = -\Delta s / (n_p g_{\max})$ allows for a change in variables with $d\nu = k dt$.¹⁷ As will be shown below, ν is related to the efficiency of the modification reaction via $\nu = -\ln(1 - \varepsilon)$ or, in the limit of small reaction efficiencies, $\nu \cong \varepsilon$.

Equations 1, 2, etc., can be solved under the assumption that at time $t = 0$ the number of pristine particle species N_1 equals the total number of particles in the system n_p . For example, integration of eq 1 yields $N_1 = n_p \exp[-g_{\max} \nu]$. This result can be used to obtain the solution of eq 2 as $N_2 = g_{\max} n_p \exp[-g_{\max} \nu] (\exp[\nu] - 1)$. Successive repetition of this process and substitution of the results yields the final expression for the normalized frequency of particles with g functional ligands

(15) Mullen, D. G.; Desai, A. M.; Waddell, J. N.; Cheng, X.; Kelly, C. V.; McNerny, D. Q.; Majoros, I. J.; Baker, J. R., Jr.; Sander, L. M.; Orr, B. G.; Banaszak Holl, M. M. *Bioconjugate Chem.* **2008**, *19*, 1748–1752.

(16) This assumption will not be entirely satisfied if reactive sites are in close proximity or functional groups are particularly space-filling (such as the grafting of high molecular mass polymer chains to the particle surface). In this case the kinetic constant is expected to decrease with each modification step depending on the geometric details of the system.

(17) The “reduced rate” parameter ν is introduced in order to render the result independent of the details of the time scale and kinetic nature of the modification process.

(i.e., the ligand distribution function) after completion of the modification process as $P(g) = N_{g+1}/n_p$, where

$$P(g) = \frac{g_{\max}!}{g!(g_{\max} - g)!} e^{-g_{\max} \nu} (e^{\nu} - 1)^g \quad (4)$$

From the definition of $P(g)$, the average value for the number of ligands per particle $\langle g \rangle$ is obtained as $\langle g \rangle = \sum_g g P(g) = g_{\max} (1 - \exp[-\nu])$. It is worthwhile to consider the relationship of eq 4 to the Poisson distribution that was used in previous studies to evaluate the distribution of ligands bound to particle (or more specifically dendrimer) systems.^{14,15} In the limit of $\nu \ll 1$, eq 4 can be rewritten as

$$P(g) \cong \frac{g_{\max}!}{(g_{\max} - g)!} e^{-\nu(g_{\max} - 1)} P_{\text{Poisson}}(g) \quad (5)$$

where $P_{\text{Poisson}}(g)$ denotes the Poisson distribution that is defined as $P_{\text{Poisson}}(g) = e^{-\nu} \nu^g / g!$.¹⁸ Equation 5 reveals that $P(g)$ reduces to the Poisson distribution if the limits $g_{\max} \rightarrow \infty$ and $(\nu g_{\max}) \rightarrow 0$ are concurrently satisfied. In reality this could correspond to, for example, large dendrimer or colloidal systems in the limit of very low coupling efficiencies (the systems analyzed in ref 14 represent such a case). Equation 5 also reveals that Poisson's distribution will become increasingly inaccurate as g_{\max} decreases (or, alternatively, νg_{\max} increases) and thus fail to describe the distribution of ligands in the case of smaller particle systems or more efficient modification reactions.^{19,20} In the following, ligand distributions will be evaluated on the basis of $P(g)$ as given by eq 4 that is preferred to the approximate distribution defined by eq 5, since the latter is valid only in the limit of $\nu \ll 1$.

Experimental Evaluation of the Ligand Distribution Function.

In order to assess the capacity of eq 4 to capture the ligand distribution of particle systems undergoing incomplete modification reactions, $P(g)$ was used to evaluate the distribution of polymer ligands in PEG-conjugated trypsin model systems. Trypsin, a protease that catalyzes the hydrolysis of peptide bonds, was chosen as a model system for several reasons: First, the rather low molecular mass of about 23.8 kDa renders trypsin accessible to quantitative experimental techniques such as matrix-assisted laser desorption ionization time-of-flight (MALDI-TOF) mass spectrometry in order to determine the distribution of polymer grafts among the modified "enzyme particles". Second, the conjugation of PEG is a widely used technique to increase the activity retention of enzymes in various pharmaceutical and nonpharmaceutical application environments and thus presents an important technological context for the present study.^{21,22}

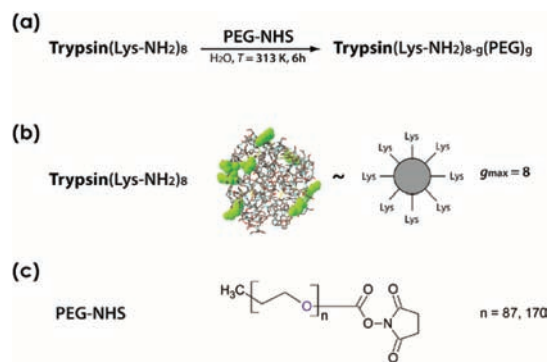


Figure 2. Illustration of the conjugated enzyme model systems and the chemical procedure for enzyme modification. (a) Reaction scheme for modification of trypsin (EC 3.4.21.4, $M \approx 23.8$ kDa, bovine pancreas) with NHS-activated poly(ethylene glycol) (PEG-NHS) with molecular mass $M = 3.5$ kDa and 7.5 kDa, respectively. The efficiency of the reaction is $\varepsilon = 0.25$ –0.43 depending on conditions (see Table 1 for details). (b) Illustration of the conformation of trypsin determined from crystal structure analysis (structure shows only carbon backbone). The positions of the eight lysine residues of the native trypsin are highlighted in green. (c) Chemical structure of poly(ethylene glycol)-*N*-hydroxysuccinimide (PEG-NHS).

Table 1. Reaction Conditions and Molecular Characteristics of Conjugated Trypsin Model Systems

sample ID	molar ratio PEG-NHS: trypsin	efficiency ε_{exp}	efficiency (calc) $\varepsilon_{\text{calc}}$
Try-PEG3500-1	10:1	0.43	0.43
Try-PEG3500-1	50:1	0.34	0.33
Try-PEG7500-1	10:1	0.26	0.29
Try-PEG7500-2	50:1	0.25	0.26

Conjugation of PEG to trypsin was accomplished by non-specific reaction of poly(ethylene glycol)-*N*-hydroxysuccinimide (PEG-NHS) with the amino functionality of lysine residues that are exposed on the protein surface.²³ The particular trypsin type used in this study (EC 3.4.21.4, bovine pancreas) exhibits eight lysine residues and thus is representative of a particle with eight reactive sites. Two series of low molecular mass PEG ($M_w = 3.5$ kDa and 7.5 kDa) were used as conjugates in order to avoid significant interactions between bound polymer ligands during the grafting reaction (a prerequisite for assumption 2; see discussion above).²⁴ The overall efficiency of the modification process was determined via a fluorescent assay (of free primary amino groups) to be in the range $\varepsilon \cong 0.25$ –0.44. The reaction procedure as well as the structure of the trypsin model (based on crystal structure analysis) is illustrated in Figure 2. In total, four model systems were synthesized with excess molar ratios of PEG-NHS of 10:1 and 50:1 for each PEG ligand. Table 1 summarizes the characteristics of the respective conjugated enzyme model systems.

Figure 3 summarizes the MALDI-TOF spectra of the native trypsin enzyme (Figure 3a), as well as the low molecular mass PEG-modified trypsin (Try-PEG3500-1, Figure 3b) that were

(18) Beichelt, F. E.; Fatti, L. P. *Stochastic Processes and Their Applications*; Taylor and Francis Inc.: New York, 2002.

(19) The deficiency of the Poisson distribution in describing ligand distributions in particlelike systems originates from the inappropriate assumptions of the reaction kinetics. In particular, it can be shown that a Poisson process results if the number of sites per particle is constant during the modification process (see, for example, ref 20). This is clearly inadequate for particle modification reactions where the number of reactive sites decreases with each ligand that is being bound to the particle surface, as shown in Figure 1. The errors associated with this assumption are expected to increase with decreasing g_{\max} and increasing νg_{\max} .

(20) Flory, P. J. *J. Am. Chem. Soc.* **1940**, *62*, 1561–1565.

(21) Klivanov, M. A. *Nature* **2001**, *409*, 241–245.

(22) Peterson, J. I.; Vurek, G. G. *Science* **1985**, *224*, 123–125.

(23) It has been demonstrated by several research groups that PEG-NHS preferentially reacts with the amino functionalities of lysine residues. Although partial functionalization of alternative amino functionalities cannot be excluded, their contribution is expected to be minor (see, for example, ref 8).

(24) If ligand interactions are predominantly of steric origin, then interactions are expected to be negligible if the hydrodynamic radius R_H of the ligand species is less than the average distance between the reactive sites on the particle surface (about 1.5 nm in the case of trypsin). Since $R_{H, \text{PEG3500}} \cong 0.5$ nm and $R_{H, \text{PEG7500}} \cong 0.8$ nm, both ligand systems are consistent with the assumption of negligible ligand interactions.

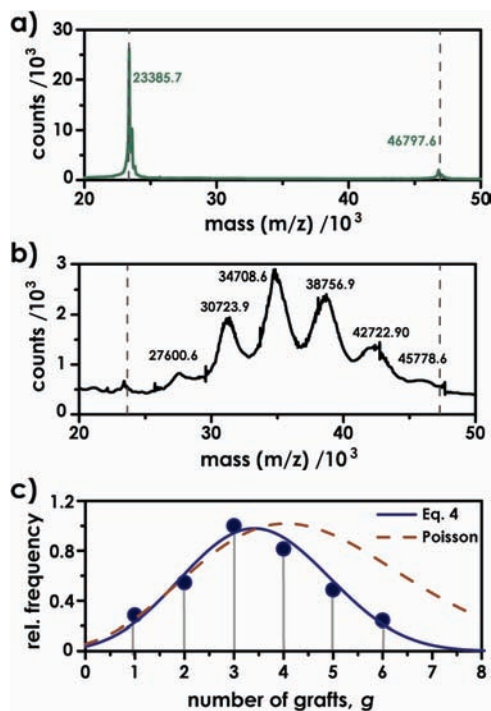


Figure 3. Characterization of the Try-PEG3500-1 model system and comparison to calculated ligand distribution function (eq 4). (a) MALDI-TOF spectrum of native trypsin (EC 3.4.21.4, bovine pancreas). Peak confirms molecular mass of $M \approx 23.8$ kDa. (b) MALDI-TOF spectrum of PEG-conjugated trypsin (Try-PEG3500-1) after dialysis. Peaks confirm partial modification with efficiency $\varepsilon = 0.43$. (c) Experimental partial frequency distribution of PEG ligands (●) obtained from spectrum b after peak fitting and correction with molecular weight of native trypsin. Solid line shows distribution calculated from eq 4 with the assumption of a total number of reactive sites $g_{\max} = 8$ per enzyme. The dotted line shows the Poisson distribution calculated from the corresponding value of ν (see text for details).

obtained from an Applied Biosystems Voyager DE-STR MALDI-TOF mass spectrometer. The peaks at mass-to-charge ratio $m/z \approx 27.6, 30.7, 34.7, 38.7,$ and 42.7 kDa indicate a distribution of the number of surface-bound ligands within 1–5 PEG ligands per trypsin (we note that peaks corresponding to double-charged species have been observed but are not shown here). Assuming that the ionic states are sufficiently long-lived (i.e., the average lifetime of ions exceeds the mean time-of-flight) allows for correlation of the amplitude of the respective peaks in the MALDI-TOF spectra with the frequency of the respective molecular species in the system (this assumption has been used successfully before in the analysis of PEG-modified proteins by means of MALDI-TOF).^{13,22,25} This leads to the frequency distribution of PEG functionalities shown in Figure 3c, from which the average degree of enzyme modification can be obtained as $\langle g \rangle_{\text{exp}} = \sum a_i g_i / \sum a_i = 3.41$, where a_i denotes the MALDI-TOF peak amplitude of trypsin species with g_i PEG ligands. Note that this corresponds to an efficiency of $\varepsilon = 0.43$ and is, within experimental error, identical to the independently determined efficiency of the modification process by use of

(25) We note that the interpretation of peak amplitudes measured by MALDI-TOF as being proportional to the frequency of the respective molecular species rests upon the assumption of sufficiently long-lived ionic species as well as linear detector sensitivity. This assumption has to be validated by independent assessment of parameters that are characteristic of the ligand distribution. In the present case, the fluorescamine method was applied to confirm the reaction efficiency concluded from the MALDI-TOF analysis (see Experimental Section).

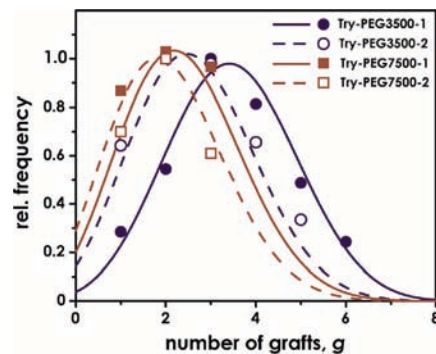


Figure 4. Comparison of experimental (symbols) and calculated (lines) frequency distributions of PEG-residues on modified trypsin model systems: (●) Try-PEG3500-1, (○) Try-PEG3500-2, (■) Try-PEG7500-1, and (□) Try-PEG7500-2. The average values of the respective experimental distributions are represented within 5% by the calculated distribution functions (see also Table 1).

fluorescamine (see above). A quantitative comparison of the experimental frequency distribution of sample Try-PEG3500-1 with eq 4 is shown in Figure 3c, revealing excellent agreement between the predicted and experimentally determined distributions of polymer ligands. The average value obtained from the best fit of $P(g)$ to the experimental data can be calculated to be identical to the experimental value, that is, $\langle g \rangle = 3.45$, thus further demonstrating the quality of agreement between the experimental and calculated distributions. The figure also reveals the key distinguishing features of eq 4 from the Poisson distribution that was used in previous studies to empirically describe the characteristics of ligand distributions in partially modified dendrimer systems. While it provides adequate agreement for $g < \langle g \rangle$, the Poisson distribution significantly overestimates the skewness of the distribution. In particular, the Poisson distribution fails to converge to zero at $g > g_{\max}$, thus allowing for the possibility of binding more ligands to a particle surface than there are available reactive sites.^{19,20}

Following the procedure outlined above, the ligand distributions of samples Try-PEG3500-2, Try-PEG7500-1, and Try-PEG7500-2 were analyzed by MALDI-TOF mass spectrometry. Figure 4 depicts the respective ligand distributions determined by MALDI-TOF along with the corresponding best fit of $P(g)$. In all cases the calculated distribution function was found to provide an adequate representation of the experimental ligand distributions. In particular, as shown in Table 1, fitting of eq 4 to the experimental data is found to reproduce the experimental grafting efficiencies within 5%.

In order to further evaluate the capacity of eq 4 to describe the distribution of bonded ligands in more diverse particlelike systems, $P(g)$ was used to calculate the ligand distribution in functionalized enzyme and dendrimer systems for which experimental data have been reported in the literature (see Figure S1 in Supporting Information).^{14,26} The excellent agreement between experimental distributions and calculated $P(g)$ obtained from the reported values for g_{\max} and ε provides additional support for the general applicability of eq 4 to capture ligand distributions in particlelike systems undergoing partial modification reactions.

Several important conclusions can be drawn from eq 4 with respect to the design of particlelike systems with well-defined (i.e., uniform) number of ligands. As shown in Figure 5a, the

(26) Drevon, G. F.; Hartleib, J.; Scharff, E.; Rueterjans, H.; Russell, A. J. *Biomacromolecules* **2001**, *2*, 664–671.

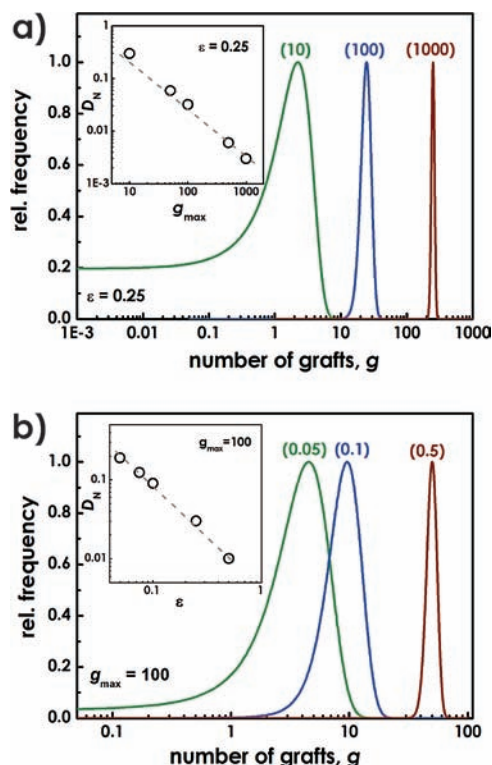


Figure 5. (a) Distribution of functional ligands for partially modified particle systems ($\varepsilon = 0.25$) calculated from eq 4 for different total numbers of reactive sites per particle: $g_{\max} = 10$ (green), 100 (blue), or 1000 (red). Distributions are normalized to peak value 1. (Inset) Decrease of the normalized variance, $D_N = (\langle g^2 \rangle - \langle g \rangle^2) / \langle g \rangle^2$, of the ligand distribution with increasing number of reactive sites per particle g_{\max} (see ref 27). The line is introduced to guide the eye. (b) Distribution of ligands calculated for a fixed particle system ($g_{\max} = 100$) for different reaction efficiencies: $\varepsilon = 0.05$ (green), 0.25 (blue), or 0.5 (red). Distributions are normalized to peak value 1. (Inset) Decrease of the normalized variance, $D_N = (\langle g^2 \rangle - \langle g \rangle^2) / \langle g \rangle^2$, of the ligand distribution with increasing reaction efficiency (see ref 27). The line is introduced to guide the eye.

relative width of $P(g)$ decreases for a given efficiency (here $\varepsilon = 0.25$) with increasing g_{\max} ; that is, the frequency of ligands per particle becomes increasingly narrowly distributed about the average value with increasing number of reactive sites per particle.²⁷ Therefore, if the number of reactive sites is small (corresponding to, for example, proteins, enzymes, or small nanoparticle systems), the relative width of the distribution of ligands is significant and thus knowledge of $P(g)$ will be important in order to understand and predict the properties of the modified particle system. In the limit of large particle sizes (with g_{\max} exceeding about 100), the particle system will be appropriately represented by assuming each particle to carry $\langle g \rangle$ functional groups. The latter case should be representative of, for example, polymer grafting reactions to inorganic particles (such as silica or gold) with particle diameters in excess of 10 nm.

The dependence of $P(g)$ on ε for constant g_{\max} (corresponding to, for example, distinct modification reactions performed with the same particle system) is shown in Figure 5b for the case of $g_{\max} = 100$. With decreasing efficiency of the modification process the relative width of the distribution is found to increase—an effect that becomes more pronounced with decreasing g_{\max} . This bears relevance for small particle systems

such as dendrimers or enzymes for which modification reactions (such as PEGylation) are typically inefficient, thus resulting in a significant fraction of unmodified particles.

Conclusion

In conclusion, we have derived and validated an analytical expression (eq 4) to capture the distribution of ligands in particle systems that are subjected to incomplete modification reactions. As expected from the law of large numbers, if the number of reactive sites per particle is large (typically this will correspond to large nanoparticle-type systems), an appropriate representation of the particle system is to consider each particle to carry a number of functional ligands that is equal to the average number for the respective particle system. For small numbers of sites per particle the distribution significantly broadens—an effect that becomes more pronounced with decreasing reaction efficiency. Thus, in order to facilitate narrow ligand distributions, large particle systems and efficient modification reactions are required. In cases where these conditions are not fulfilled, knowledge of the distribution should be important in order to understand and predict the functional activity of modified particle systems. Since the treatment of ligand binding is applicable to a wide array of modified particlelike systems such as proteins, enzymes, and dendrimers as well as inorganic nanocrystals, the presented results should aid the design of synthesis conditions for modified particle and particlelike systems in which better control of functional activity is facilitated by tailoring of the ligand distribution. Current studies focus on the extension of the approach to capture the effect of steric hindrance on the binding of ligands to particle surfaces as well as the evaluation of the impact of ligand distributions on the bioactivity of modified enzyme systems.

Experimental Section

Materials. Trypsin (Try) from bovine pancreas (EC 3.4.21.4, $M \approx 23.8$ kDa), poly(ethylene glycol)-*N*-hydroxysuccinimide (PEG-NHS, $M_w = 3.5$ kDa), sodium tetraborate, calcium chloride, sinapinic acid, and trinitrobenzenesulfonate were purchased from Aldrich and used without prior purification (unless indicated otherwise).

Sample Preparation. Prior to modification, trypsin was dialyzed in buffer solution (aqueous solution of sodium tetraborate, 10 mM, and calcium chloride, 5 mM) at pH 8 for 12 h prior to use. For the low-molecular weight PEGylated trypsin Try-PEG3500-1, the modification was as follows: 1.5 mg of PEG-NHS was added to 2 mL of a buffer solution of trypsin ($c = 0.5$ mg/mL), and the mixture was vigorously stirred for 2 h at $T = 40$ °C (this approach corresponds to a 10-fold excess of PEG-NHS with respect to available lysine residues). Unreacted PEG-NHS was separated by dialysis for 12 h against buffer solution. Dialysis was performed by use of Amicon Diaflo PM-10 membrane with molecular weight cutoff 10 000 (Amicon Inc., Beverly, MA). No trypsin was detected within the permeate. Following dialysis, the reaction product was stored at $T = -20$ °C for long-term stability. Analogous reaction procedures were applied for a molar ratio (PEG-NHS:trypsin) = 50:1 (representing sample Try-PEG3500-2) as well as for the higher molecular weight analogues Try-PEG7500-1 [corresponding to molar ratio (PEG-NHS:trypsin) = 10:1] and Try-PEG7500-2 [corresponding to molar ratio (PEG-NHS:trypsin) = 50:1], respectively. The grafting efficiency for all reactions was evaluated by both fluorescamine and MALDI-TOF analysis (details are provided below). The characteristics of all trypsin conjugates are summarized in Table 1.

Physical Characterization. Fluorescamine reactions were performed at $T = 25$ °C by addition of the dialyzed enzyme sample to fluorescamine solution buffer (50 mM borate, pH 8). Sample

(27) An analytical expression for the normalized variance can be derived from eq 4 as $(\langle g^2 \rangle - \langle g \rangle^2) / \langle g \rangle^2 = 1 / (g_{\max} (\exp[\nu] - 1))$.

fluorescence was determined on a Cary Eclipse fluorescence spectrophotometer.

MALDI-TOF mass spectrometry was performed on an Applied Biosystems Voyager DE-STR mass spectrometer (mass range 1–400 000 Da) equipped with positive and negative ion modes, linear and reflector modes, and a nitrogen laser operating at $\lambda = 337$ nm. In a typical sample preparation protocol, 0.23 mg of trypsin or PEG-modified trypsin samples and 10 mg of sinapinic acid (matrix) were each dissolved in 1 mL of water/acetonitrile (70/30) (corresponding to a ratio analyte/matrix = 1/5000). Sample and matrix were deposited on sample holders (stainless steel, Biosystems) by successive drop casting of 1 μ L of the respective matrix and enzyme solution and subsequent solvent evaporation.

Acknowledgment. Financial support by the Defense Threat Reduction Agency (via Contract HDTRA1-09-1-0014) and the Air Force Office for Scientific Research (via Grant FA9550-09-1-0169) as well as the Petroleum Research Fund governed by the American Chemical Society is gratefully acknowledged. We also thank G. Berry (Department of Chemistry) and M. Bier (Center for Molecular Analysis at Carnegie Mellon University) for helpful discussions.

Supporting Information Available: One figure showing analysis of literature data on ligand distributions in modified dendrimer and enzyme systems. This material is available free of charge via the Internet at <http://pubs.acs.org>.

JA107139C